Available online at www.sciencedirect.com
SCIENCE DIRECT
Journal of Catalysis 229 (2005) 24–29
JOURNAL OF CATALYSIS
www.elsevier.com/locate/jcat

Effect of diffusion in catalytic dehydration of alcohol over silica–alumina with continuous macropores

Ryoji Takahashi *, Satoshi Sato *, Toshiaki Sodesawa, Kazuya Arai, Miyuki Yabuki

Department of Applied Chemistry, Faculty of Engineering, Chiba University, Yayoi, Inage, Chiba 263-8522, Japan

Received 27 July 2004; revised 8 October 2004; accepted 14 October 2004

Abstract

Bimodal porous silica–alumina catalysts with both continuous macropores and mesopores were prepared from tetraethyl orthosilicate in the presence of polyethylene oxide, and the effectiveness of macropores in vapor-phase dehydration of 2-propanol was evaluated by the comparison with silica-alumina having no macropores. The reaction rate of dehydration varies depending on the particle size and the presence of macropores as well as reaction temperature. For more detail data processing, diffusion coefficients in pores at each reaction temperature were theoretically calculated by assuming molecular diffusion and Knudsen diffusion for catalysts with and without macropores, respectively. Then, we compare the catalyst effectiveness factors obtained experimentally with the theoretical curve. The experimental data well agree with theoretical prediction. The results clearly show that the macropores with interconnected structure effectively work as pathways for rapid diffusion and improve the reaction kinetics.

Keywords: Silica–alumina; Bimodal pores; Diffusion; Macropores; Catalyst effectiveness factor; Sol–gel

1. Introduction

Diffusion in pores of solid catalysts during catalytic reaction sometimes affects the overall kinetics of reaction. In chemical industry, practical catalysts are formed in spheres, pellets, rods, and so on, with typical size of 5–10 mm, whereas catalyst powders or particles smaller than 1 mm are usually tested in laboratory. Diffusion limitation has been frequently observed in the industrial catalysts with large particle size, whereas has rarely attracted an attention in the catalysts used in laboratory-scale reactor except for the liquid phase reaction [1–9]. Because of the recent progress in catalyst preparation, however, catalytic results suggesting the decrease in activity by diffusion limitation have been reported for newly developed catalysts with high activity even in laboratory-scale gas-phase reaction [10–12]. Diffusion of gas molecules in mesopores smaller than a mean free path is described with Knudsen equation [13]

$$D = \frac{2}{3} r_{\mathrm{p}} \left(\frac{8RT}{\pi M} \right)^{1/2}, \tag{1}$$

where D, r_{p}, R, T, and M are respectively diffusion coefficient in pores, pore radius, gas constant, temperature, and molecular weight of gas molecules. The smaller the mesopore size is, the smaller the diffusion coefficient becomes. A time, t, necessary to diffuse particular length, l, is roughly estimated by the relation [14]

$$t = l^2/2D. \tag{2}$$

Therefore, long time is required for gas molecules to move into the center of catalyst particles with large size and with small mesopores in which diffusion coefficient is also small. Then, the center portion of catalyst particles does not effectively work in reaction, when the reaction rate is very fast. The catalyst effectiveness factor, E_{f}, is defined as [13]

$$E_{\mathrm{f}} = \frac{\text{real reaction rate}}{\text{ideal reaction rate}}. \tag{3}$$

* Corresponding authors. Fax: +81-43-290-3376.
E-mail addresses: rtaka@faculty.chiba-u.jp (R. Takahashi), satoshi@faculty.chiba-u.jp (S. Sato).

0021-9517/$ – see front matter
doi:10.1016/j.jcat.2004.10.010

The ideal reaction rate is that without suffering the effect of diffusion. An excellent catalyst is expected to show both high reaction rate and $E_f = 1$. This can be achieved only by increasing diffusion rate in pores of catalysts with large particle size.

One of the methods to increase the diffusion rate of molecules in the catalyst is to provide macropores in it [15–18]. Usual catalysts have only mesopores and/or micropores in which diffusion of molecules is strongly restricted. Presence of macropores in the catalyst has an effect to enhance the diffusion rate, as predicted from Knudsen equation (Eq. (1)). Furthermore, a recent simulation study reveals that well-designed arrangement of macropores with high connectivity is much more effective for high catalytic performance than random configuration of macropores, as observed in most of commercially available catalysts [19]. It was, however, difficult to design such pore configuration in practical catalysts by the conventional catalyst preparation methods. Recently, we have developed silica-based bimodal porous catalysts with both macropores and mesopores, such as Ni/SiO_2 [20], silica–zirconia [21,22] and silica–alumina [11,12]. In the catalysts, the macropores are formed by freezing transitional structures of phase separation induced in a sol–gel solution [23]. The macropores have 3-dimensional high connectivity without neck structure, and can be used as pathways for mass flow of liquid and gas phases [24,25]. In our latest work, acceleration of diffusion of nitrogen gas by the presence of macropores has been also recognized at −196 °C for the material prepared by the same methodology [26]. We propose that the catalysts prepared by the methodology to provide macropores by freezing transitional structure of phase separation are the new generation of bimodal porous catalysts because of the presence of 3-dimensionally interconnected macropores instead of randomly distributed macropores.

In the preliminary catalytic test of silica–alumina thus prepared in cracking of cumene, high catalytic activity was observed for the catalysts with macropores when the reaction rate was fast, and we related the observation with the enhancement of diffusion due to the presence of macropores [11,12]. However, such effect has not been quantitatively evaluated. In this work, we prepared two different silica–alumina catalysts with and without macropores, where other structural features are essentially the same. The catalytic dehydration of 2-propanol was used as a model reaction, and effect of the presence of macropores on the overall reaction kinetics was evaluated from the change in catalyst effectiveness factor.

2. Experimental

The silica–alumina catalysts were prepared as reported previously [11,12], using tetraethyl orthosilicate (TEOS, Shinetsu) and aluminum nitrate nonahydrate ($Al(NO_3)_3 \cdot 9H_2O$, Wako) as sources of silica and alumina, respectively. Either of the polyethylene oxides (PEO) with molecular weight of 100 000 (PEO100) or 3 000 (PEO3) were added in the sol–gel preparation of catalysts. Nitric acid was used as a catalyst of sol–gel reaction. The obtained silica–alumina catalysts prepared in the presence of PEO100 and PEO3 were named SA100 and SA3, respectively. A commercial silica–alumina catalyst, N631L, was used for the comparison of catalytic activity. The obtained silica–alumina catalysts were grounded to two sizes, 2.0 and 0.2 mm, and distinguished with -L and -S in notification, respectively.

Scanning electron microscope (SEM, SM200, Topcon, Japan) was used to observe micrometer scale morphology of the samples. Nitrogen adsorption–desorption isotherm was measured at −196 °C on an OMNISORP 100CX (Beckman Coulter, USA). Specific surface area and mesopore volume were calculated by the BET method and from the amount of nitrogen adsorbed at $P/P_0 > 0.95$, respectively. Size distribution of pores smaller than 50 nm was calculated using the Dollimore–Heal method. Temperature-programmed desorption (TPD) of ammonia and 2,6-dimethylpyridine (2,6-DMP) adsorbed at 200 °C was measured to estimate the acidic property of the catalysts. Details of the characterization are described elsewhere [12].

The catalytic dehydration of 2-propanol was carried out in a fixed-bed flow reactor made with glass at temperatures between 140 and 220 °C. Catalyst bed with 0.15 g was heated to the reaction temperature. Then, 2-propanol was fed into the reactor at the rate of 8.0 $cm^3\ h^{-1}$ as a liquid, together with 30 $cm^3\ min^{-1}$ He carrier gas. The effluent was analyzed with an on-line gas chromatograph equipped with TCD and 1 m-length Benton + DNP column.

3. Results and discussion

3.1. Structures and catalytic activity of silica–alumina catalysts

In the preparation of silica–alumina gel by the sol–gel method, no interaction was detected between aluminum cation and silica as long as the reaction was carried out in acidic conditions at moderate temperature [12]. That is, aluminum cations dissolve in solution as hydrated cations rather than being incorporated in silica network, and the aluminum cations aggregate as a salt during drying. Therefore, the sol–gel-derived silica–alumina is not so active in catalysis. The addition of PEO in the preparation drastically increases the catalytic activity of the resultant silica–alumina [12]. PEO chain with a large number of ether oxygen atoms can interact with both silica surface and aluminum cations. Therefore, we have speculated that such interaction increases the dispersion of aluminum cations in the silica–alumina, leading to the high activity. This effect is expected for both PEO100 and PEO3. In addition, PEO100 has another effect to induce phase separation just before gelation. Then, transitional structure of phase separation is frozen as permanent micrometer scale morphology.

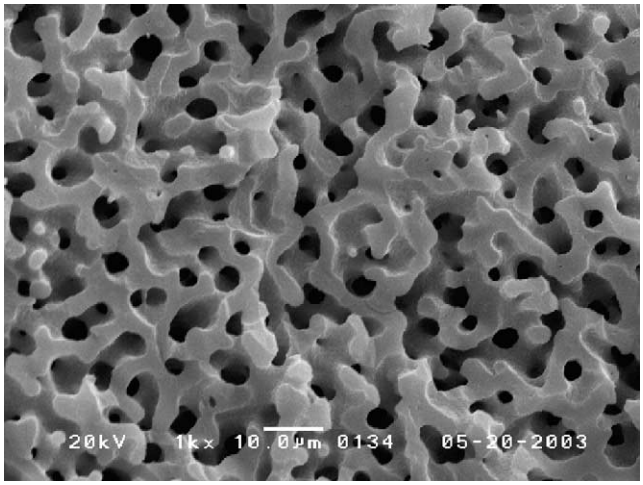

Fig. 1. SEM image of fractured surface of SA100.

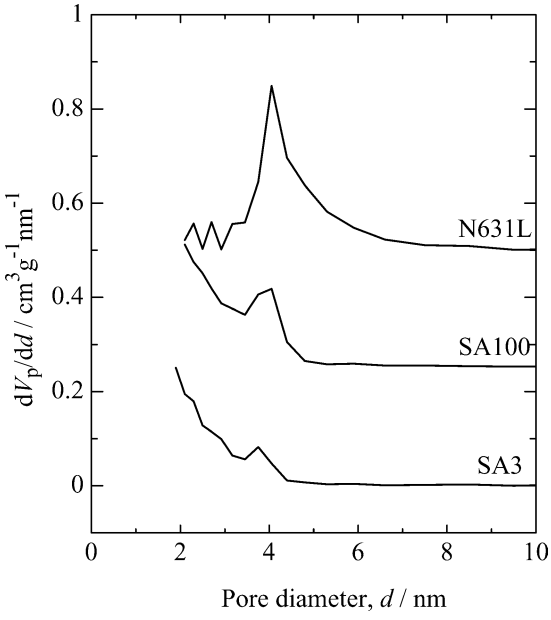

Fig. 2. Pore size distribution curves calculated from nitrogen adsorption isotherms.

Figure 1 shows the SEM image of silica–alumina prepared in the presence of PEO100. Macropores with uniform size of ca. 3 μm, which are interconnected 3-dimensionally, are observed. This structural feature is essentially the same as that reported previously [11,12], and we can assure that the macropores are formed by phase separation. In pore size distribution measured by mercury porosimetry, this sample shows a sharp peak in micrometer size range as shown previously [11]. The sample prepared with PEO3 has no macropores and nothing was observed with SEM at this magnification.

Figure 2 shows the pore size distribution calculated from nitrogen adsorption. The reference catalyst, N631L, shows a peak at 4 nm while other samples show no peak suggesting the presence of small mesopores together with micropores. Structural features of the catalysts are summarized in Table 1. Both SA100 and SA3 show similar structural features of specific surface area and mesopore size, although SA100 has somewhat larger specific surface area. The similarity in mesoscale structure between SA100 and SA3 is probably resulted from the same kind of interaction between silica and organic additives, PEO100 and PEO3: hydrogen bonding between silanols on silica and ether oxygens in PEO [12]. In TPD, the amount of adsorbed ammonia is a measure of total acid amount while that of 2,6-DMP is a measure of number of Brønsted acid sites [12]. It is recognized that number of Brønsted acid on N631L is much smaller than that on SA100 and SA3. The difference between SA100 and SA3 is relatively small. These results assure us that the major difference between SA100 and SA3 is the presence of macropores in SA100.

Table 1
Additives in preparation and structural properties of catalysts[a]

	Additive	Specific surface area ($m^2\ g^{-1}$)	Pore volume ($cm^3\ g^{-1}$)		Base adsorbed[b] ($\mu mol\ g^{-1}$)	
			Meso	Macro	NH_3	2,6-DMP
SA100[c]	PEO100	620	0.388	0.870	250	215
SA3[c]	PEO3	429	0.276	–	250	170
N631L	–	347	0.438	0.150	250	100

[a] These data were taken from Refs. [11,12].
[b] Amount of base adsorbed at 200 °C.
[c] Preparation compositions are TEOS:aluminum nitrate:water:60% HNO_3:PEO = 9.31:2.21:11.5:1.15:x in weight ratio, where x is 1.15 for SA100 and 2.00 for SA3.

Figures 3 and 4 show the changes in conversion of 2-propanol and selectivity to propene with reaction temperature. Conversion increases simply with reaction temperature, while the values at each temperature vary depending on the catalyst used. The SA100 shows higher activity than the commercial catalyst, N631L, at any temperature (Fig. 3). In addition, selectivity to propene is higher than that of N631L. The major by-product over N631L is dipropyl ether. Larger mesopores in N631L than in the sol–gel catalysts would make possible the two-molecule dehydration reaction. Difference in the ratio of Brønsted acid to the total acid would be also the origin of the difference in the selectivity. Regarding the effect of the presence of macropores, there is small difference in conversion between the SA100 and SA3 at lower reaction temperature (Fig. 4). SA100 has larger specific surface area and larger amount of Brønsted acid than SA3. Therefore, it would be expected that SA100 shows somewhat higher activity even at the low reaction temperature. However, the catalytic result suggests that the difference in catalytic ability between SA100 and SA3 is not so large. In the cracking of cumene, both SA100 and SA3 showed similar activity at low reaction temperature [12], which is similar to the present results on dehydration of 2-propanol. With rising reaction temperature, conversion over SA100 becomes higher than SA3. Furthermore, it is recognized that powdered catalyst shows higher conversion than one particle for each catalyst series. Because the activation energy of reaction is larger than that of diffusion, reaction

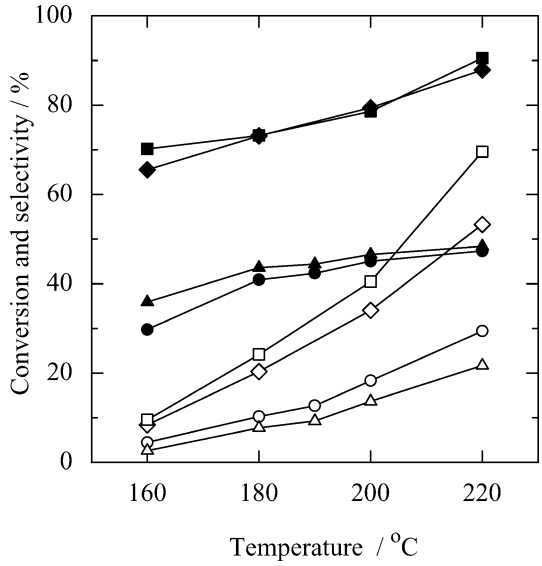

Fig. 3. Changes in 2-propanol conversion (open symbols) and selectivity to propene (closed symbols) with reaction temperature. Square: SA100-S, rectangular: SA100-L, circle: N631L-S, triangle: N631L-L.

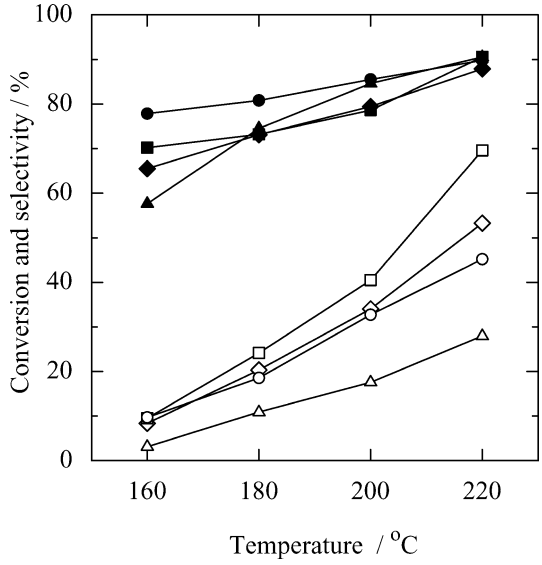

Fig. 4. Changes in 2-propanol conversion (open symbols) and selectivity to propene (closed symbols) with reaction temperature. Square: SA100-S, rectangular: SA100-L, circle: SA3-S, triangle: SA3-L.

rate increases more rapidly with reaction temperature than diffusion rate. Therefore, the diffusion limitation tends to be significant at high reaction temperature. There is no contradiction to consider that the cause of the difference in conversion at high temperature is the result of acceleration of diffusion by the presence of macropores in SA100.

3.2. Quantitative evaluation of the effectiveness of macropores

We have obtained the catalytic results suggesting the diffusion limitation in pores of catalysts even in the laboratory-scale reaction. Then, we quantitatively evaluate the effectiveness of macropores. The apparent first-order reaction rate constant, k, can be calculated according to

$$k = \frac{F_0}{V}\left\{-y_0 x + (1+y_0)\ln\frac{1}{1-x}\right\} \tag{4}$$

for fixed-bed flow reactor [13]. Here, F_0, V, y_0, and x are volumetric feed rate of reactant, volume of catalyst bed, molar ratio of reactant in the feed gas, and conversion. The obtained rate constants are summarized in Table 2. Here, it should be noted that the data contains the effect of diffusion.

Table 2
First order reaction rate constant for dehydration of 2-propanol and theoretical diffusion coefficients in mesopores and macropores

Temperature (°C)	k[a] (s^{-1})				$D_{ideal} \times 10^7$ ($m^2\,s^{-1}$)	
	SA100-S	SA100-L	SA3-S	SA3-L	Mesopores[b]	Macropores[c]
160	0.61	0.53	0.62	0.19	3.67	135
180	1.83	1.49	1.34	0.74	3.76	144
200	3.78	2.97	2.82	1.31	3.84	154
220	9.94	6.01	4.63	2.40	3.92	164

[a] Calculated from reaction data shown in Fig. 3 by using Eq. (4).
[b] Calculated by using Eq. (1). $r_p = 2V_{meso}/A = 1.3$ nm was used in the calculation.
[c] Calculated by using Eq. (5). $\sigma = 0.5$ nm and $\Omega = 1$ were used in the calculation.

Diffusion coefficient of molecules in the catalysts without macropores can be calculated using Knudsen equation (Eq. (1)). Here, we have to consider the diffusion both of reactant, 2-propanol, and products, propene and dipropyl ether. Because the selectivity to dipropyl ether is about one-tenth of that to propene, we used an average molecular weight of 2-propanol and propene in Eq. (1). Regarding the pore radius, we use $2V_{meso}/A$ as mesopore radius assuming straight cylinder-type pores, where V_{meso} and A are mesopore volume and specific surface area, because no clear peak is observed in pore size distribution curve calculated from nitrogen adsorption isotherm (Fig. 2). It should be noted that the specific surface area calculated with the BET method contains some errors due to the presence of micropores. However, $2V_{meso}/A$ would be the most reliable as an experimentally obtained pore radius. On the other hand, it is clear that the size of macropores in SA100 is much larger than average free path of gas molecules, typically in the order of 0.1 μm. Therefore, the diffusion coefficient in SA100 is evaluated assuming the molecular diffusion. For the estimation of diffusion coefficient in macroporous samples, therefore, we used the following equation for molecular diffusion [13]:

$$D = 0.0018583\frac{T^{3/2}(1/M_A + 1/M_B)^{1/2}}{P\sigma_{AB}^2\Omega_{AB}}, \tag{5}$$

where P, σ, Ω are respectively total pressure, Lennard-Jones potential parameter, and collision integral. Use of this

equation would be appropriate for the SA100 sample because its macropores not are randomly distributed but are 3-dimensionally interconnected without neck. Table 2 summarizes diffusion coefficients calculated for mesopores and macropores at different reaction temperatures. Both diffusion coefficients for Knudsen diffusion and for molecular diffusion increase with reaction temperature, while coefficient of molecular diffusion is about 40 times larger than that of Knudsen diffusion. In addition, we have to take into account the contribution of structural factors such as porosity, ε, and tortuosity, τ, to diffusion in a real porous material [13]:

$$D_{\text{pore}} = \frac{\varepsilon}{\tau} D_{\text{ideal}}. \tag{6}$$

For SA3, porosity of 0.38 is obtained from pore volume shown in Table 1 and density of silica (2.2 g cm^{-3}). For SA100, porosity affecting the molecular diffusion would be the volume ratio of macropores, and it becomes 0.51. The tortuosity for usual porous material is 3–6 [13]. Then, we can evaluate that the factor ε/τ is in the range of 0.13–0.063 for SA3 and 0.17–0.085 for SA100. Thus, the real diffusion coefficients in porous materials are about 10 times smaller than the ideal values. We use 1/10 of diffusion coefficient listed in Table 2 as D_{pore} in the following data processing.

It is theoretically predicted that catalyst effectiveness factor for spherical samples is described by [13]

$$E_{\text{f}} = \frac{3}{m}\left\{\frac{1}{\tanh(m)} - \frac{1}{m}\right\}. \tag{7}$$

Here m is the Thiele modulus expressed as

$$m = r_{\text{sphere}}\sqrt{\frac{k_{\text{ideal}}}{D}}, \tag{8}$$

where r_{sphere} and k_{ideal} are respectively radius of catalyst particles and reaction rate constant without restriction of diffusion. Assuming that no diffusion limitation occurs in the powdered SA100-S with macropores, k for the sample at each reaction temperature can be regarded as k_{ideal}, which can be used to obtain Thiele modulus using Eq. (8). Furthermore, the ratio of k/k_{ideal} at the same temperature provides catalyst effectiveness factor of respective catalyst,

$$E_{\text{f}} = \frac{k}{k_{\text{ideal}}} = \frac{3}{m}\left\{\frac{1}{\tanh(m)} - \frac{1}{m}\right\}. \tag{9}$$

Then, we can compare the catalyst effectiveness factors obtained experimentally with theoretical ones.

Figure 5 shows the change in catalyst effectiveness factor with Thiele modulus for all the reaction data except for N631L. Because N631L has different pore structures and shows different product selectivities compared with SA100, factors other than diffusion would be incorporated in the k/k_{ideal}. In the plot, data points are located between 0.01 and 10 in m, and E_{f} decreases with increasing m at $m > 0.2$. Because of small m in powdered macroporous silica–alumina, SA100-S, the assumption that no diffusion limitation occurs

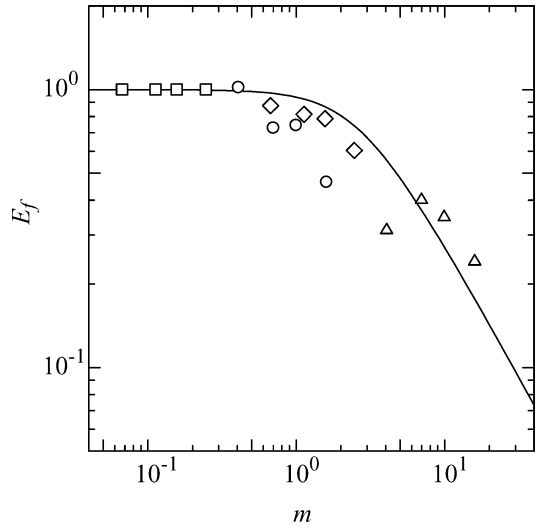

Fig. 5. Change in catalyst effectiveness factor, E_{f}, with Thiele modulus, m, in the 2-propanol dehydration over SA100 and SA3 catalysts. Data in Table 2 were used in calculation of E_{f} and m for the data points, assuming there was no diffusion effect in the reaction over SA100-S. The symbols are the same as those in Fig. 4. The solid curve is theoretically calculated for spheres.

in it is appropriate. In the figure, a theoretical E_{f} curve calculated using Eq. (9) is also drawn. All the data points well fit the theoretical curve. This result ensures that the causes of the differences in catalytic activity at high reaction temperature between SA100 and SA3 and those between particles and powders of the same catalysts are attributed to the diffusion limitations in SA3 without macropores and in large particles, respectively. The effectiveness of macropores is clearly shown for the catalyst with large particle size, as expected.

The m in the present data is limited up to transition region between reaction limitation and diffusion limitation. Therefore, the ratio of E_{f} between SA100-L and SA3-L particles with size of 2 mm is limited to 3. Since m for the reaction over catalyst with larger size is in the diffusion limitation region, effectiveness of macropores would be more significant in experiments using a catalyst with larger particle size. Unfortunately, these experiments are very difficult in laboratory-scale reaction because of limited diameter of reactor.

We have to mention estimated errors in the data processing. We used diffusion coefficients calculated theoretically assuming Knudsen diffusion in mesopores and molecular diffusion in macropores. These values could somewhat deviate from real ones due to both limitation in the equations and parameters used. Furthermore, we postulate the same ε/τ value of 0.1 for both SA100 and SA3. The values of τ would vary depending on the pore structure. Use of D_{pore} values obtained experimentally at each temperature rather than theoretical values would lead to more exact comparison, if one could measure them directly. Inevitably, distribution in particle size in the samples would be a cause of an error. Thus,

the plot in Fig. 5 may contain substantial errors along the x-axis, although the general trend prevails.

4. Conclusion

Two types of silica–alumina catalysts with and without macropores were prepared by the sol–gel method using PEO with different molecular weight. They showed higher catalytic activity than a commercial silica–alumina catalyst, N631L, in dehydration of 2-propanol. In addition, effectiveness of macropores in the reaction is quantitatively clarified by comparing catalyst effectiveness factor for the reaction using the catalysts with controlled particle sizes. The catalyst effectiveness factor obtained experimentally well agrees with theoretical prediction. The results clearly indicate that the macropores with well-designed structure effectively work as pathways for rapid diffusion and improve the reaction kinetics.

References

[1] H. Saito, Shokubai (Japanese) 1 (1959) 32.
[2] J. Wood, L.F. Gladden, Chem. Eng. Sci. 57 (2002) 3033.
[3] Y. Nitta, T. Imanaka, S. Terahashi, J. Catal. 80 (1983) 31.
[4] U.K. Singh, R.N. Landau, Y. Sun, C. LeBlond, D.G. Blachmond, S.K. Tanielyan, R.L. Augustine, J. Catal. 154 (1995) 91.
[5] Y. Sun, J. Wang, C. LeBlond, R.N. Landau, D.G. Blachmond, J. Catal. 161 (1996) 759.
[6] T. Nakayama, K. Yamashiro, S. Sato, F. Nozaki, Appl. Catal. A 151 (1997) 437.
[7] S. Sato, R. Takahashi, T. Sodesawa, F. Nozaki, X.-Z. Jin, S. Suzuki, T. Nakayama, J. Catal. 191 (2000) 261.
[8] H. Tsai, S. Sato, R. Takahashi, T. Sodesawa, S. Takenaka, Phys. Chem. Chem. Phys. 4 (2002) 3537.
[9] R. Takahashi, S. Sato, T. Sodesawa, T. Ikeda, Phys. Chem. Chem. Phys. 5 (2003) 2476.
[10] A. Shichi, A. Satsuma, M. Iwase, K. Shimizu, S. Komai, T. Hattori, Appl. Catal. B 17 (1998) 107.
[11] R. Takahashi, S. Sato, T. Sodesawa, M. Yabuki, J. Catal. 200 (2001) 197.
[12] M. Yabuki, R. Takahashi, S. Sato, T. Sodesawa, K. Ogura, Phys. Chem. Chem. Phys. 4 (2002) 4830.
[13] J.M. Smith, in: Chemical Engineering Kinetics, third ed., McGraw-Hill Book Co, New York, 1981, Ch. 11.
[14] J. Crank, The Mathematics of Diffusion, second ed., Oxford University Press, Oxford, 1975, Ch. 2.
[15] N. Wakao, J.M. Smith, Chem. Eng. Sci. 17 (1962) 825.
[16] A. Leitao, M. Dias, A. Rodrigues, Chem. Eng. J. 55 (1994) 81.
[17] T. Numaguchi, K. Shoji, Shokubai (Japanese) 42 (2000) 63.
[18] T. Numaguchi, Catal. Surveys Japan 5 (2001) 59.
[19] U.A. El-Nafaty, R. Mann, Chem. Eng. Sci. 54 (1999) 3475.
[20] N. Nakamura, R. Takahashi, S. Sato, T. Sodesawa, S. Yoshida, Phys. Chem. Chem. Phys. 2 (2000) 4983.
[21] R. Takahashi, K. Nakanishi, N. Soga, J. Ceram. Soc. Japan 106 (1998) 772.
[22] R. Takahashi, S. Sato, T. Sodesawa, K. Suzuki, M. Tafu, K. Nakanishi, N. Soga, J. Am. Ceram. Soc. 84 (2001) 1968.
[23] K. Nakanishi, J. Porous Mater. 4 (1997) 67.
[24] H. Minakuchi, K. Nakanishi, N. Soga, N. Ishizuka, N. Tanaka, J. Chromatogr. A 797 (1998) 121.
[25] R. Takahashi, S. Sato, T. Sodesawa, A. Haga, H. Nishino, J. Ceram. Soc. Japan 112 (2004) 99.
[26] Y. Tomita, R. Takahashi, S. Sato, T. Sodesawa, M. Otsuda, J. Ceram. Soc. Japan 112 (2004) 491.